

SCIENTIFIC REPORTS



OPEN

Cyclodextrin-Based Metal-Organic Nanotube as Fluorescent Probe for Selective *Turn-On* Detection of Hydrogen Sulfide in Living Cells Based on H₂S-Involved Coordination Mechanism

Received: 04 November 2015

Accepted: 19 January 2016

Published: 25 February 2016

Xuelian Xin¹, Jingxin Wang², Chuanfang Gong¹, Hai Xu², Rongming Wang¹, Shijie Ji¹, Hanxiao Dong¹, Qingguo Meng³, Liangliang Zhang¹, Fangna Dai¹ & Daofeng Sun¹

Hydrogen sulfide (H₂S) has been considered as the third biologically gaseous messenger (gasotransmitter) after nitric oxide (NO) and carbon monoxide (CO). Fluorescent detection of H₂S in living cells is very important to human health because it has been found that the abnormal levels of H₂S in human body can cause Alzheimer's disease, cancers and diabetes. Herein, we develop a cyclodextrin-based metal-organic nanotube, CD-MONT-2, possessing a {Pb₁₄} metallamacrocycle for efficient detection of H₂S. CD-MONT-2' (the guest-free form of CD-MONT-2) exhibits *turn-on* detection of H₂S with high selectivity and moderate sensitivity when the material was dissolved in DMSO solution. Significantly, CD-MONT-2' can act as a fluorescent *turn-on* probe for highly selective detection of H₂S in living cells. The sensing mechanism in the present work is based on the coordination of H₂S as the auxochromic group to the central Pb(II) ion to enhance the fluorescence intensity, which is studied for the first time.

Hydrogen sulfide (H₂S), a colourless toxic gas with rotten egg smell, possesses double-sided nature¹. On the one hand, H₂S is known as a dangerous industrial pollutant for many years². Because of the properties of forming explosive mixtures in the air, and causing an explosion under fire or heat, the H₂S gas has received a growing universal attention in the aspect of safety^{3,4}. On the other hand, along with nitric oxide (NO) and carbon monoxide (CO), the H₂S gas has been recognized as a third gaseous transmitter gas in the human body recently⁵. *In vivo*, H₂S is generated by endogenous enzymes^{6–8} (such as, cystathionine β-synthase (CBS), cystathionine γ-lyase (CSE), or 3-mercaptopyruvate sulfurtransferase (MPST)) in many organs (e.g., heart, brain, kidneys, nervous system, etc.) and tissues (e.g., adipose tissues, etc.)^{9–12}. The abnormal levels of generated H₂S were related to Alzheimer's disease, cancers, diabetic complications and Down's syndrome^{13–15}. Hence, more and more attention has been drawn to the sensitive and selective detection of H₂S which is chosen as a target in biological systems¹⁶.

In the past decade, a variety of fluorescent probes were developed for rapid detection of H₂S. Generally, the design strategies are highly dependent on the chemical properties of the physiologically active species^{17,18}. On the basis of current research, the sensing mechanism for the fluorescent probes of H₂S detection can be classified into three types^{19–22}: (i) H₂S reductive reactions; (ii) H₂S nucleophilic reactions and (iii) metal sulfide precipitation reactions. Most of reported results are focused on design and synthesis of organic molecules with desired functional groups to detect H₂S based on^{23–25} (i) and (ii) reactions, seldom are metal-organic frameworks (MOFs)

¹State Key Laboratory of Heavy Oil Processing, China University of Petroleum (East China), Qingdao Shandong 266580, China. ²Centre for Bioengineering and Biotechnology, China University of Petroleum (East China), Qingdao 266580, China. ³Chemistry & Chemical and Environmental Engineering College, Weifang University, Weifang 261061, Shandong Province, China. Correspondence and requests for materials should be addressed to D.S. (email: dfsun@upc.edu.cn)

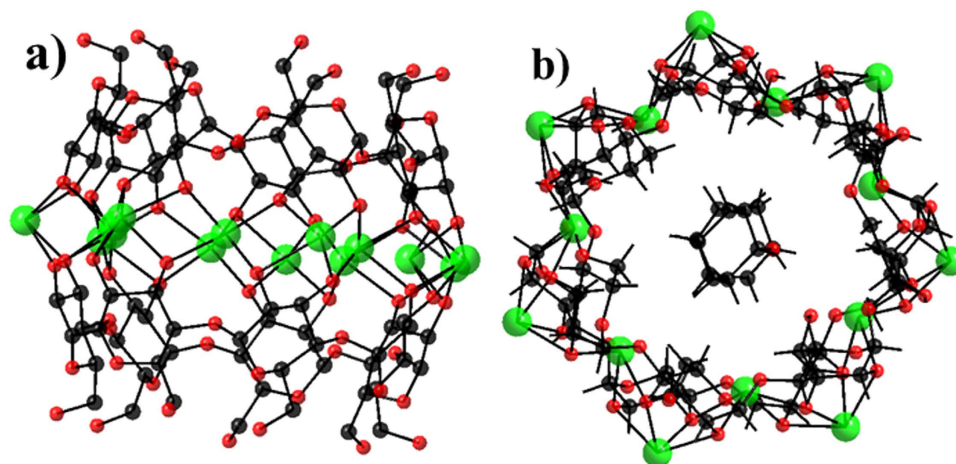


Figure 1. Structure of CD-MONT-2. (a) Side view of the structure of CD-MONT-2 (the hydrogen atoms and cyclohexanol molecules are omitted for clarity, green: Pb(II), black: C and red: O). (b) Top view of the structure of CD-MONT-2, showing the fourteen-nuclearity lead metallamacrocycle and the uncoordinated cyclohexanol molecules in the cavity (the hydrogen atoms are omitted for clarity, green: Pb(II), black: C and red: O).

or metal-organic nanotubes (MONTs). In general, MOFs or MONTs with both high selectivity and fluorescence *turn-on* in response to H_2S are very rare^{17,26,27}.

In the previous work, we described a cyclodextrin-based Pb(II) metal-organic nanotube (CD-MONT-2) exhibiting temperature-dependent fluorescence and adsorption of I_2 molecules²⁸. The excellent fluorescent property of CD-MONT-2 and the high affinity of Pb(II) to S atom prompted us to study its potential in fluorescent detection of H_2S . Herein, we report CD-MONT-2' (the guest-free sample of CD-MONT-2) as a fluorescence *turn-on* probe for H_2S detection. Significantly, CD-MONT-2' can detect H_2S in living cells with high selectivity and moderate sensitivity. Furthermore, in the present work, a new sensing mechanism that H_2S molecules act as auxochromic groups to interact with the central chromophore to enhance the fluorescence emission is discovered for the first time, which is quite different from previous results.

Results and Discussion

Structure of CD-MONT-2. Colorless crystals of CD-MONT-2 were obtained under the guidance of reference²⁸. The cyclodextrin-based Pb(II) metal-organic nanotube (CD-MONT-2) consists of coplanar $\{\text{Pb}_{14}\}$ metallamacrocycle surrounded by two β -cyclodextrin molecules, as shown in Fig. 1. In the CD-MONT-2, the dimensions of the chiral cavity are ca. $13.0 \times 10.3 \times 10.2 \text{ \AA}$ filled with cyclohexanol molecules. The uncoordinated solvates in the cavity can be fully removed by heating CD-MONT-2 at 120°C for half an hour to generate guest-free form, CD-MONT-2'. The phase purity of bulk sample was further confirmed by comparison of the powder X-ray diffraction (PXRD) patterns of as-synthesized and activated sample (Supplementary Figure S1), which matched well with the simulated PXRD pattern from the single-crystal data. The following fluorescent measurements were based on CD-MONT-2'.

Fluorescent measurements of CD-MONT-2'. CD-MONT-2' is slightly soluble in dimethylsulphoxide (DMSO), in which CD-MONT-2' emits fluorescence at 409 nm ($\Phi = 0.02$) upon the excitation at 330 nm (Supplementary Figure S2). To probe the fluorescent response of CD-MONT-2' towards H_2S , CD-MONT-2' was dissolved in DMSO to make a $10 \mu\text{M}$ stock solution, then the emission spectrum was recorded from 350 to 650 nm upon the excitation at 330 nm. CD-MONT-2' in DMSO solution exhibits relatively weak fluorescence and keeps in the *turn-off* state due to the very dilute concentration. However, with the addition of H_2S (1 mL) into the above solution, the fluorescence intensity shows a significant increase with time. Compared to the original one, almost 15 fold fluorescence enhancement is observed after 15 minutes, and no further increase occurs (Fig. 2a). The time-dependent fluorescence measurements for the addition of H_2S into the stock solution reveal that CD-MONT-2' in DMSO exhibits rapid response toward H_2S , which is different from the reported Pb-based complexes²⁹. To further probe the fluorescence *turn-on* response to sulfide, various concentrations of Na_2S (0– $10 \mu\text{M}$) were added to the stock, and the fluorescence spectra were recorded in Fig. 2b. Similarly, the fluorescence intensity clearly increases with the increasement of the concentration of Na_2S , and almost becomes 4 times of original fluorescence intensity when the concentration of Na_2S reaches $10 \mu\text{M}$.

In order to confirm the fluorescent selectivity to Na_2S over other substances, various additional experiments were carried out by gradual addition of other sodium salts (such as Na_2SO_4 , $\text{Na}_2\text{S}_2\text{O}_3$, Na_2SO_3 , NaNO_3 , NaHCO_3 , NaCl , NaClO , NaOAc , FeCl_2 , FeCl_3 and KH_2PO_4), reducing agents (glucose), thiol amino acids (GSH and L-cys), non-thiol amino acids (Gln, L-Thr, L-Trp, L-Tyr, Leu, L-Leu, L-asp and Gly), reactive nitrogen species (NO_2^-), reactive oxygen species (H_2O_2 and $^t\text{BuOOH}$), and reactive sulfur species (TGA, THU and thiophene)^{30,31}. And the spectra are shown in supplementary Figure S3–S5. The blank of only β -cyclodextrin in DMSO at $10 \mu\text{M}$ with Na_2S was also recorded, and the spectrum is shown in supplementary Figure S3o. The fluorescence intensities of $(I-I_0)/I_0$ (where I_0 is the initial fluorescence intensity, and I is the fluorescence intensity after the addition of the analyte) spectra ($\lambda = 409 \text{ nm}$) are displayed in Fig. 2c,d. The results reveal that the additions of those substances

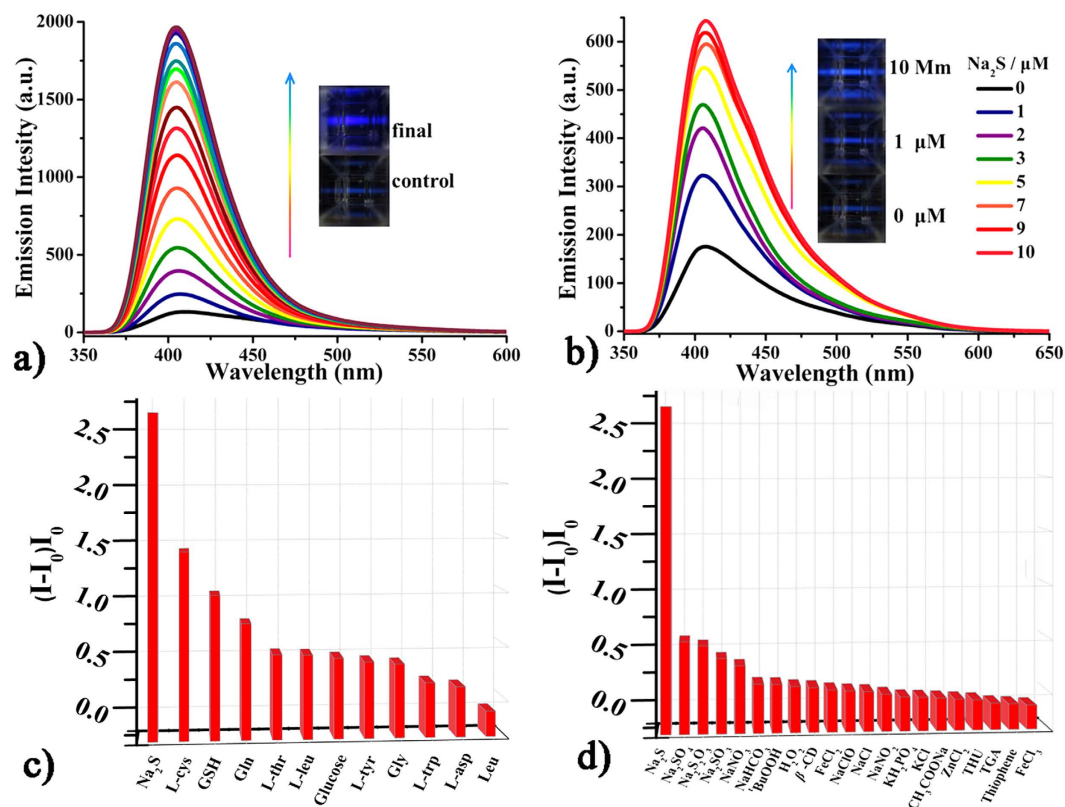


Figure 2. Fluorescent spectra of 10 μM CD-MONT-2' in DMSO treated with different substances.

(a) Addition of H_2S after 15 min and the insert pictures were taken under Xe lamp before and finally treated with H_2S after 15 min. (b) Continual addition of Na_2S and the insert pictures were taken under Xe lamp. (c) Fluorescent intensity of $(I-I_0)/I_0$ (409 nm) spectra with 10 μM Na_2S , 10 mM glucose and amino acids. (d) Fluorescent intensity of $(I-I_0)/I_0$ (409 nm) spectra with 10 μM Na_2S , inorganic salts, RNS, ROS and RSS.

have little effect on the fluorescence intensity of CD-MONT-2', indicating the high selectivity to Na_2S over other substances through fluorescence enhancement. All these results demonstrate that CD-MONT-2' exhibits fluorescence *turn-on* response to H_2S molecule with high selectivity and moderate sensitivity¹¹.

Sensing mechanism. In the past decade, several MOF-based fluorescence *turn-on* probes on the detection of H_2S were reported¹⁹. The reported sensing mechanism is mostly based on the H_2S -involved organic reactions, through which the *turn-off* state of those material can be converted to *turn-on* state. Hence, there always exists a desired functional group in the MOF materials that can react with H_2S to complete the conversion. However, in the metal-organic nanotube of CD-MONT-2', there is no additional organic functional groups that can react with H_2S to enhance the fluorescence emission. Therefore, the sensing mechanism in the present work should be different with the previous results. It is known that cyclodextrins are nonaromatic and fluorescence silent, as a result, the fluorescence emission of CD-MONT-2' should be assigned to a metal-centered transition involving the *s* and *p* orbitals of Pb(II) ions^{28,32}. Thus, the fluorescence enhancement should derive from the interactions between H_2S molecules and Pb(II) ions due to the high affinity of S atom to Pb(II) ion (K_{sp} of PbS: 1×10^{-28})³³. As an auxochrome, the coordination of H_2S to Pb(II) ion significantly increases the fluorescence emission of CD-MONT-2' (Fig. 3).

To further confirm the above sensing mechanism, the UV-Vis absorbance spectra, FTIR spectra and ¹H NMR spectra were recorded for CD-MONT-2' in DMSO before and after addition of H_2S . The absorption band of CD-MONT-2' in DMSO appears at around 266 nm ($\epsilon = 5.68 \times 10^4 \text{ M}^{-1} \text{ cm}^{-1}$), which could be assigned to the transition from $6s^2$ to $6sp$ involving the lone pairs on the Pb(II)³⁴. When H_2S was added into the DMSO solution containing CD-MONT-2', the absorption band enhances and shows a red-shift (Fig. 4a), which may be derived from the attachment of "S" to Pb(II)³⁴. As a common auxochrome and donor, the connection of "S" could always shift the absorption to a longer wavelength and increase the absorption intensity³⁵⁻³⁷. In contrast, the addition of other substances only enhances the absorption intensity slightly and shows almost no shift. These results indicate that the sensing mechanism for CD-MONT-2' is based on the coordination of S atom to Pb(II) to increase the electron transfer to enhance the fluorescence intensity³⁸⁻⁴².

Moreover, the FTIR spectra of CD-MONT-2' in DMSO solution before and after treated with H_2S or Na_2S were carried out (Fig. 4b). The absorption peaks remain unchanged, except that there is a slight difference around 1250 cm^{-1} . The broad peak around 3450 cm^{-1} can be assigned to the stretching vibration of adsorbed water and hydroxyl groups in β -CD molecule. The peak around 1655 cm^{-1} is attributed to the O-H bending vibration of

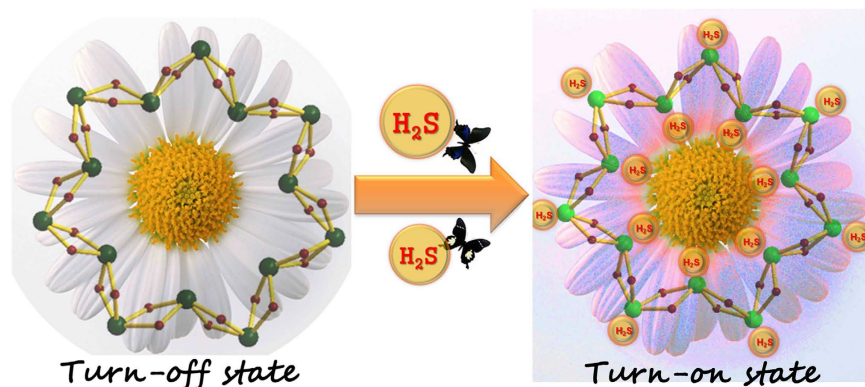


Figure 3. The possible mechanism for the *turn-on* fluorescent probe of CD-MONT-2'. The Figure is drawn by Xuelian Xin.

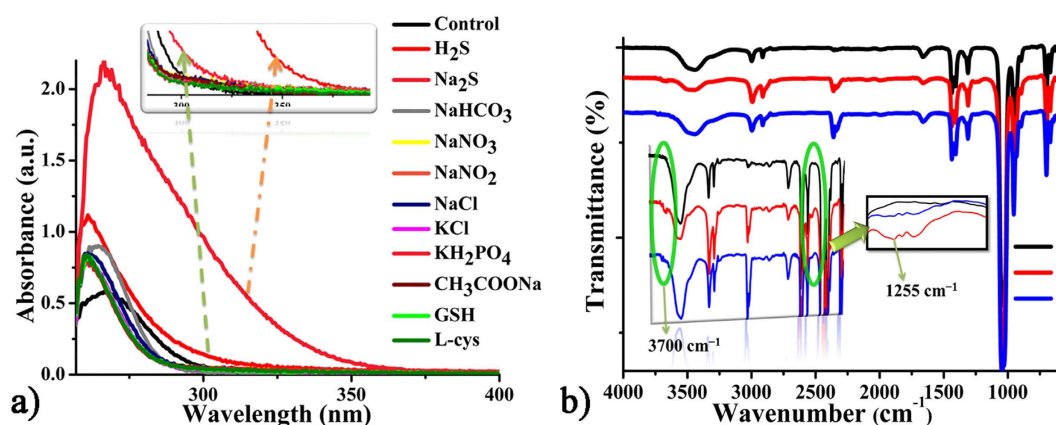


Figure 4. (a) UV-vis spectra of 10 μM CD-MONT-2' in DMSO treated with H_2S and 10 μM different substances; (b) FTIR spectra of 10 μM CD-MONT-2' in DMSO with, (1) none, (2) H_2S and (3) 10 μM Na_2S ; The insert spectra are the enlarged view of the new peaks.

adsorbed water and hydroxyl groups in β -CD molecule. The absorption peak around 1033 cm^{-1} is stretching vibration of C–O–C and C–O bonds in the hole^{28,43–45}. Moreover, new weak distinct peaks appeared around 1255 cm^{-1} and 3700 cm^{-1} . The former peaks at about 1255 cm^{-1} can be assigned to the stretching vibration of Pb–S bond, further indicating the formation of new chemical bond (Pb–S bond)^{46–48}, the latter peaks around 3700 cm^{-1} can be assigned to the relatively free hydroxyl group with weak hydrogen bond⁴⁹. In addition, the ^1H NMR spectra before and after the addition of H_2S are shown in Supplementary Figure S6. Compared with the original one of CD-MONT-2', new peaks at 7.95 ppm, 2.89 ppm and 2.73 ppm are observed in the spectra of CD-MONT-2' treated with H_2S . The new peaks should be assigned to the SH which involved in the coordination or free H_2S ^{36,50}.

Cellular imaging experiments. The *turn-on* fluorescence sensing of H_2S by CD-MONT-2' prompted us to perform its potential in selective *turn-on* detection of H_2S in living cells. To explore the fluorescent efficiency and selective response of CD-MONT-2' towards H_2S in the complex biological systems, CD-MONT-2' in DMSO was diluted by PBS (phosphate buffer solution, 10 mM, pH = 7.4, the spectra are shown in Supplementary Figure S7 and the fluorescent spectra in different pH values diluted by PBS are shown in Supplementary Figure S8) at a concentration of 0.1 μM . The fluorescence measurements reveal that about 6 fold fluorescence enhancement is observed for CD-MONT-2' in PBS buffer after 10 minutes upon the addition of H_2S (1 mL), indicating the response toward H_2S (Fig. 5a). Similarly, the fluorescence intensity obviously increases with the increase of Na_2S , and becomes almost 4 times of original fluorescence intensity when the concentration of Na_2S reaches 10 μM (Fig. 5b, detection limit 0.058 μM , the figure is shown in Supplementary Figure S9). Moreover, in order to confirm the fluorescent selectivity, various additional experiments were carried out by gradual addition of other inorganic salts (such as NaNO_3 , NaHCO_3 , NaClO , FeCl_2 , FeCl_3 and KH_2PO_4), reducing agents (glucose), thiol amino acids (GSH and L-cys, which are known to reduce to generate *off-target* H_2S detection under the action of enzymes⁵¹), non-thiol amino acids (Gln, L-Thr, L-Trp, L-Tyr, Leu, L-Leu, L-asp and Gly), reactive nitrogen species (NO_2^- and ONOO^-), reactive oxygen species (H_2O_2 and tBuOOH), reactive sulfur species (TGA, THU and thiophene) into CD-MONT-2' in DMSO diluted by PBS, and the spectra are shown in Supplementary Figure S10–11. The blank of only β -cyclodextrin in DMSO diluted by PBS at 10 μM with Na_2S and the interference experiments

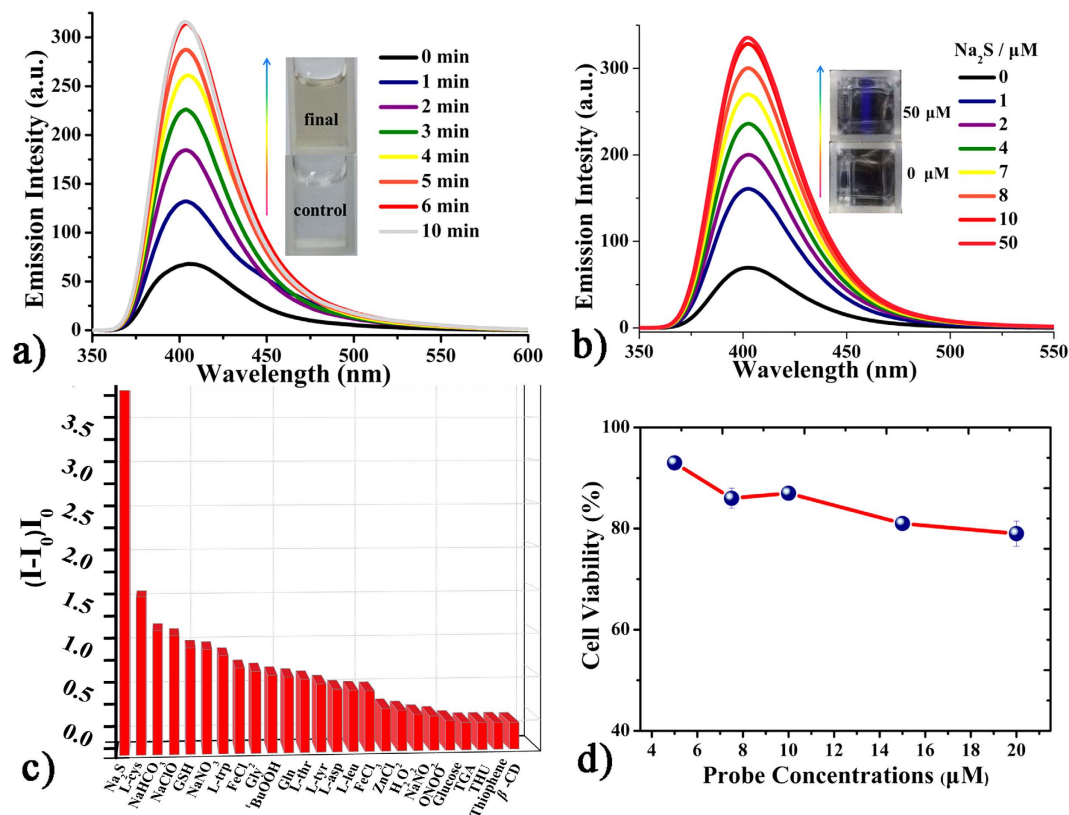


Figure 5. Fluorescent spectra of 0.1 μM CD-MONT-2' in PBS buffer (10 mM, pH 7.4, 1% DMSO) treated with, (a) H_2S after 10 min, the insert pictures were taken before and finally treated with H_2S for 10 min. (b) Continual addition of Na_2S ; the insert picture was taken in equipment under Xe lamp. (c) fluorescent intensity of $(I-I_0)/I_0$ (405 nm) spectra; (d) MTT assay of HeLa cells in the presence of different concentrations of CD-MONT-2'.

were also recorded, and the spectra are shown in Supplementary Figure S10 o and Figure S12 respectively. The results demonstrate that CD-MONT-2' exhibits fluorescence *turn-on* response to H_2S molecule in the cell growth environment with high selectivity and moderate sensitivity, possessing the potential in real-time intracellular H_2S imaging.

Hence, the CD-MONT-2' may be utilized to living cell imaging to sulphide. To test the viability and proliferation of the living cell, the MTT assay on HeLa cells was performed⁵⁰ (Fig. 5d). The cell viability is not lower than 80% until the concentration of CD-MONT-2' reaches 20 μM , indicating the low toxicity at the concentration of 0.1 μM . The HeLa cells were incubated with 10 μM probe for 15 minutes at 37 $^\circ\text{C}$ in a 5% CO_2 atmosphere, and washed with PBS for three times to remove the residual probe. Then fresh PBS containing various concentrations of Na_2S were respectively added into the treated HeLa cells and incubated for 15 minutes. The fluorescent image of control one shows that CD-MONT-2' probe could enter inside the cell and result in the weak blue fluorescent signal. However, with the increase of sulphide (Na_2S) concentration from 1 to 100 μM , the signal intensity increases obviously (Fig. 6). The strong blue fluorescent signal is observed when the sulphide concentration reaches 100 μM . These results confirm that CD-MONT-2' is active as a probe for sulphide and can be applied in living cell imaging.

In addition to supplementing cells with extraneous sources of sulphide, our experiments further focus on biothiols, such as the amino acid glutathione (GSH) and L-cysteine (L-cys), which can act as potential sulphide sources^{51–55}. After 15 minutes of incubation, addition of both thiol species (200 μM GSH or L-cys in PBS) elicits a brighter fluorescent response (see Fig. 7). The significant responses indicate that the CD-MONT-2' probe could detect not only external sulphides supplemented to the cell cultures, but also sulphides produced by the cells *in vivo*.

Discussion

The design and synthesis of fluorescent *turn-on* probes for rapid detection of H_2S in living cells is an active field in material chemistry and cell biology^{9,17}. The development of coordination chemistry in the past decades opened a new avenue in searching fluorescent materials for selective detection of H_2S . Actually, most of fluorescent coordination complexes including metal-organic frameworks show *turn-off* response towards H_2S ²⁹, functional coordination complex-based probes with fluorescent *turn-on* response towards H_2S are quite rare. Up to date, several MOF-based fluorescent *turn-on* probes have been synthesized and applied in the detection of H_2S based on reduction/precipitation mechanism¹⁹. In the present work, the sensing mechanism is based on the coordination of H_2S (as auxochromic group) to Pb(II) ion to enhance the fluorescent emission. To the best of

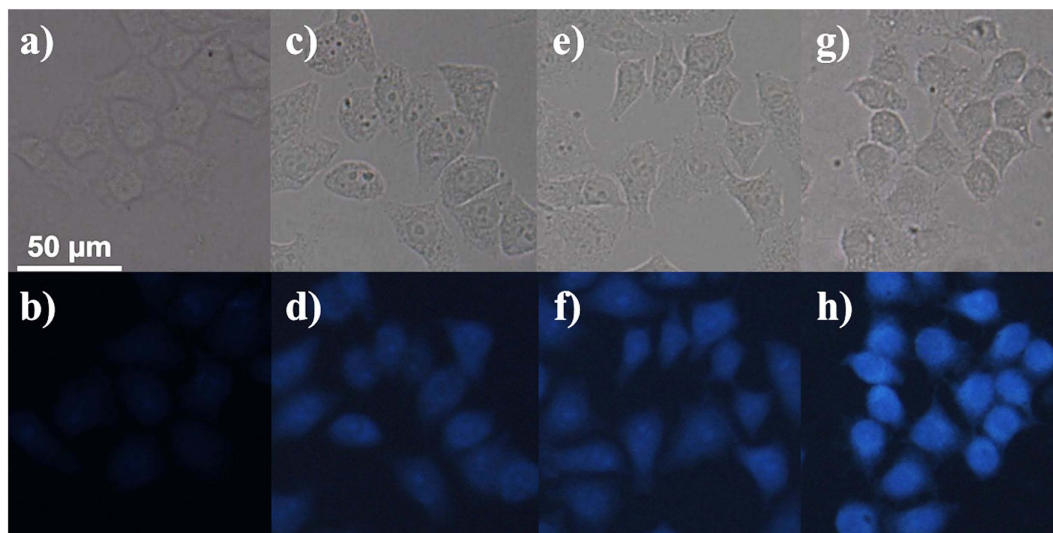


Figure 6. The fluorescent images of HeLa cells containing **CD-MONT-2'** incubated with increasing concentrations of Na_2S for 15 min at 37°C : (b) $0\ \mu\text{M}$, (d) $1\ \mu\text{M}$, (f) $50\ \mu\text{M}$, and (h) $100\ \mu\text{M}$; (a,c,e,g) are the bright field images of (b,d,f,h).

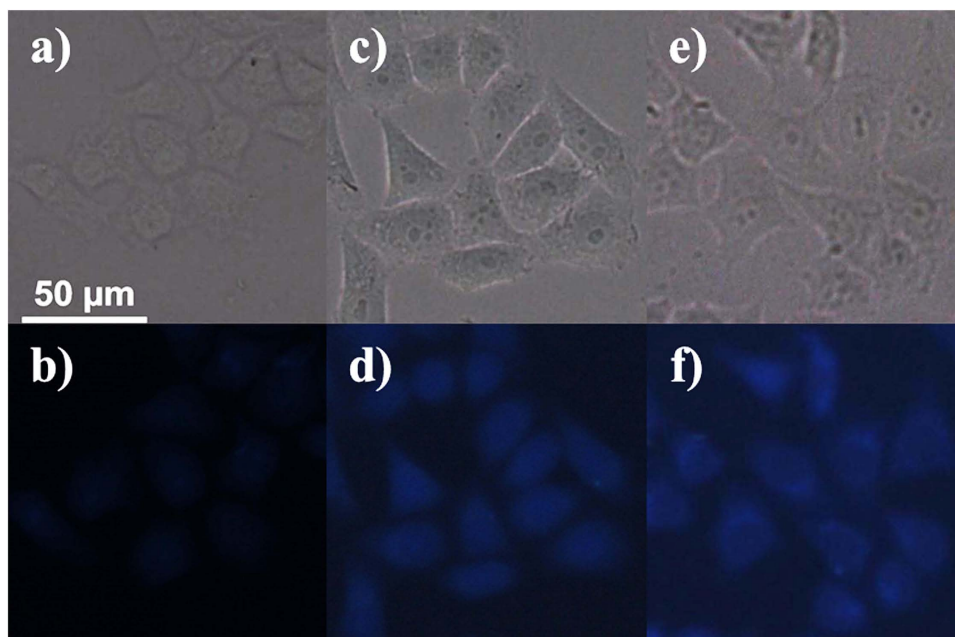


Figure 7. The fluorescent images of HeLa cells containing **CD-MONT-2'** incubated with the concentrations of (b) $0\ \mu\text{M}$, (d) $200\ \mu\text{M}$ GSH and (f) $200\ \mu\text{M}$ L-cys after 15 min at 37°C ; (a,c,e) are their bright field images of (b,d,f), respectively.

our knowledge, this is the first fluorescence *turn-on* probe that can selectively detect H_2S in living cells based on H_2S -involved coordination mechanism.

On the other hand, one of the significant bottlenecks in detection of H_2S in living cells is the toxicity of the fluorescent probe. Most of organic ligands used in the assembly of coordination complexes or metal-organic frameworks are limited to non-renewable petrochemical feedstocks and somewhat toxic. Recently, Stoddart and co-workers reported a series of MOFs composed of an edible natural product, γ -cyclodextrin⁵⁶⁻⁵⁹. In our work, **CD-MONT-2'** was assembled by use of β -cyclodextrin, which is non-toxic and increases its practical application in the fluorescent detection of H_2S in living cells.

Conclusions

In conclusion, a fluorescent metal-organic nanotube based on β -cyclodextrin for the detection of H_2S has been developed and described. The newly developed fluorescent probe can detect H_2S through fluorescence *turn-on*

fashion with high selectivity and moderate sensitivity. Furthermore, the sensing mechanism is based on the coordination of H₂S to the central metal ions of the probe to tune the fluorescence intensity, which is quite different from the results reported previously. Significantly, the use of nontoxic β -cyclodextrin ligand in the probe makes it more advantage in the practical application. Our study may provide a new way in design and synthesis of new functional material on fluorescence *turn-on* detection of H₂S in living cells.

Methods

Materials and Physical Measurements. *Materials.* All chemicals and solvents were purchased and used as received without further purification. Water used in living cell experiments were processed with a Millipore Milli-Q system (18.2 M Ω -cm). Thioglycolic acid (TGA) and thiourea (THU) were purchased. 'BuOOH could also be used to induce ROS in biological systems³¹. The ONOO⁻ source was generated by the reaction of H₂O₂, H₂SO₄, NaNO₂ and MnO₂. The concentration is obtained by UV-Vis at 302 nm⁶⁰.

Physical Measurements. Fluorescence spectra were recorded with a Hitachi F-7000 fluorescence spectrophotometer. The powder X-ray diffraction data were obtained on a Philips X' Pert with Cu-K α radiation ($\lambda = 0.15418$ nm). FTIR spectra were collected on a Bruker VERTEX-70 spectrometer in the 4000 – 600 cm⁻¹ region. The optical absorption spectra were measured on a UV-vis spectrometer (Specord 205, Analytik Jena) in the range of 200 to 600 nm. ¹H NMR spectra were recorded on a Bruker AVANCE-400 NMR Spectrometer in d₆-DMSO.

Synthesis of CD-MONT-2. β -CD (0.10 mmol, 115 mg) and PbCl₂ (0.80 mmol, 225 mg) were suspended in distilled water (30 mL) and stirred at 80 °C for an hour. After cooled to room temperature, the precipitate was separated from the mixture. The obtained solution was transformed to five 6 mL of glass tubes, then 3 mL cyclohexanol and trimethylamine were layered onto the solution in each tube. The glass tubes were sealed and heated at 110 °C for 3 days. A lot of colourless rod-like crystals were collected by filtration, washed with distilled water and dried in air (yield: 78%).

Fluorescent experiments. All fluorescent measurements were carried out at room temperature on a Hitachi F7000 fluorescence spectrophotometer. Samples were excited at 330 nm with the excitation and emission slit widths set at 20 and 10 nm, respectively. The emission spectrum was scanned from 350 to 650 nm with 1200 nm min⁻¹. The photomultiplier voltage was set at 400 V. Accordingly, the probe was dissolved in dimethylsulphoxide (DMSO) to make a 10 μ M stock solution and the added substances were dissolved in DMSO as well. The stock was diluted by PBS for 100 times to obtain the concentration of 0.1 μ M and the added substances were dissolved in PBS. The H₂S was made by the reaction of FeS and H₂SO₄ and collected in the 250 mL flask for more than 30 min. To test the time-dependent properties, 1 mL H₂S gas was taken out from the flask and bubbled into 1 mL corresponding solution.

MTT Cytotoxicity assay. HeLa cells were grown up in DMEM media with 10% FBS and penicillin/streptomycin. Cells were allowed to grow to 80% confluency before being collected using trypsin. Cells were transferred into a 96-well plate (Corning), and then incubated overnight at 37 °C in a 5% CO₂ atmosphere. A serial dilution on CD-MONT-2' was performed in DMEM media, with 10 μ L added to each well to give final concentrations of 5, 7.5, 10, 15 and 20 μ M probe. Cells were allowed to incubate for 24 h. Wells containing only cells and only DMSO were also set up to serve as positive and negative controls. To test cell viability and proliferation, the MTT assay was performed. Briefly, after incubation for the indicated times, 10 μ L of MTT solution (5 mg/mL) was added to each well, and the cells were incubated for further 4 h at 37 °C. The precipitated formazan was dissolved in 150 μ L of dimethyl sulfoxide. The absorbance at 490 nm (A490) was measured using a microplate autoreader (Molecular Devices, M2e). Note that the wells without cells acted as the blank during the A490 measurement.

Cellular imaging experiments. HeLa cells were grown as previously described. The cells were seeded onto 12 mm sterile coverslips in a 24-well plate (Corning) and allowed to grow to 80% confluency at 37 °C in a 5% CO₂ atmosphere. At this time, a final concentration of 0.1 μ M CD-MONT-2' was added to the cells and incubated for 15 minutes at the previous conditions. Media was then removed, and PBS was added to remove the probe left in solution and optimize the background signal. The sulphur source was then added (Na₂S, GSH, or L-cys) to the desired concentration and cells were incubated for 10–15 minutes at room temperature before imaging. And then, the cells were fixed for 20 min in 200 μ L 4% paraformaldehyde (the fluorescent images of HeLa cells without being fixed are showed in Figure S13). After fixation, the cells were washed thrice with PBS. The coverslip with fixed cells was topped by a glass slide with a drop of 10 μ L of glycerol/PBS (v/v = 1:1) and placed above the objective on a fluorescence microscope.

All imaging experiments were performed on a Leica DMI3000B Inverted fluorescence microscopic. Excitation and emission were monitored using blue filter provided with the scope. Imaging was performed with the \times 20 dry objectives which are provided with the scope. Images were captured using Leica Application Suite software.

References

1. Sasakura, K. *et al.* Development of a Highly Selective Fluorescence Probe for Hydrogen Sulfide. *J. Am Chem Soc.* **133**, 18003–18005 (2011).
2. Bai, P. P. *et al.* Initiation and Developmental Stages of Steel Corrosion in Wet H₂S Environments. *Corrosion Sci.* **93**, 109–119 (2015).
3. Liu, C. *et al.* Capture and Visualization of Hydrogen Sulfide by a Fluorescent Probe. *Angew. Chem. Int. Ed.* **50**, 10327–10329 (2011).
4. Wang B. S. *et al.* A reversible fluorescence probe based on Se-BODIPY for the redox cycle between HClO oxidative stress and H₂S repair in living cells. *Chem. Commun.*, **49**, 1014–1016 (2013).
5. Kabil, O. & Banerjee, R. Redox Biochemistry of Hydrogen Sulfide. *J. Biol. Chem.* **285**, 21903–21907 (2010).

6. Stipanuk, M. H. & Ueki, I. Dealing with Methionine/Homocysteine Sulfur: Cysteine Metabolism to Taurine and Inorganic Sulfur. *J. Inherit. Metab. Dis.* **34**, 17–32 (2011).
7. Kimura, H. Hydrogen Sulfide: Its Production, Release and Functions. *Amino Acids.* **41**, 113–121 (2011).
8. Li, H. *et al.* A Malonitrile-Functionalized Metal-Organic Framework for Hydrogen Sulfide Detection and Selective Amino Acid Molecular Recognition. *Sci. Rep.* **4**, 4366–4370 (2014).
9. Wu, Z. *et al.* Fluorogenic Detection of Hydrogen Sulfide Via Reductive Unmasking of *o*-Azidomethylbenzoyl-Coumarin Conjugate. *Chem. Commun.* **48**, 10120–10122 (2012).
10. Zhang, L. *et al.* Selective Detection of Endogenous H₂S in Living Cells and the Mouse Hippocampus Using a Ratiometric Fluorescent Probe. *Sci. Rep.* **4**, 5870–5878 (2014).
11. Huo, F. *et al.* Highly Selective Fluorescent and Colorimetric Probe for Live-Cell Monitoring of Sulphide Based On Bioorthogonal Reaction. *Sci. Rep.* **5**, 8969–8973 (2015).
12. Zong, C. *et al.* A New Type of Nanoscale Coordination Particles: Toward Modification-Free Detection of Hydrogen Sulfide Gas. *J. Mater. Chem.* **22**, 18418–18425 (2012).
13. Mao, G. *et al.* High-Sensitivity Naphthalene-Based Two-Photon Fluorescent Probe Suitable for Direct Bioimaging of H₂S in Living Cells. *Anal. Chem.* **85**, 7875–7881 (2013).
14. Koide, Y. *et al.* Development of a Si-Rhodamine-Based Far-Red to Near-Infrared Fluorescence Probe Selective for Hypochlorous Acid and its Applications for Biological Imaging. *J. Am. Chem. Soc.* **133**, 5680–5682 (2011).
15. Petrucci, J. F. D. S. & Cardoso, A. A. Sensitive Luminescent Paper-Based Sensor for the Determination of Gaseous Hydrogen Sulfide. *Anal. Methods.* **7**, 2687–2692 (2015).
16. Fiorucci, S. *et al.* The Third Gas: H₂S Regulates Perfusion Pressure in Both the Isolated and Perfused Normal Rat Liver and in Cirrhosis. *Hepatology.* **42**, 539–548 (2005).
17. Horcajada, P. *et al.* Metal-Organic Frameworks in Biomedicine. *Chem. Rev.* **112**, 1232–1268 (2012).
18. Kenmoku, S. *et al.* Development of a Highly Specific Rhodamine-Based Fluorescence Probe for Hypochlorous Acid and its Application to Real-Time Imaging of Phagocytosis. *J. Am. Chem. Soc.* **129**, 7313–7318 (2007).
19. Yu, F., Han, X. & Chen, L. Fluorescent Probes for Hydrogen Sulfide Detection and Bioimaging. *Chem. Commun.* **50**, 12234–12249 (2014).
20. Liu, J. *et al.* Selective Ag(I) Binding, H₂S Sensing, and White-Light Emission from an Easy-to-Make Porous Conjugated Polymer. *J. Am. Chem. Soc.* **136**, 2818–2824 (2014).
21. Ma, Y. *et al.* Heterogeneous Nano Metal-Organic Framework Fluorescence Probe for Highly Selective and Sensitive Detection of Hydrogen Sulfide in Living Cells. *Anal. Chem.* **86**, 11459–11463 (2014).
22. Yu, Q. *et al.* Dual-Emissive Nanohybrid for Ratiometric Luminescence and Lifetime Imaging of Intracellular Hydrogen Sulfide. *ACS Appl. Mater. Inter.* **7**, 5462–5470 (2015).
23. Dai, Z. *et al.* Ratiometric Time-Gated Luminescence Probe for Hydrogen Sulfide Based on Lanthanide Complexes. *Anal. Chem.* **86**, 11883–11889 (2014).
24. Zhou, X. *et al.* Recent Progress On the Development of Chemosensors for Gases. *Chem. Rev.* **115**, 7944–8000 (2015).
25. Mai, L. *et al.* Single β -AgVO₃ Nanowire H₂S Sensor. *Nano. Lett.* **10**, 2604–2608 (2010).
26. Lippert, A. R., New, E. J. & Chang, C. J. Reaction-Based Fluorescent Probes for Selective Imaging of Hydrogen Sulfide in Living Cells. *J. Am. Chem. Soc.* **133**, 10078–10080 (2011).
27. Chan, J., Dodani, S. C. & Chang, C. J. Reaction-Based Small-Molecule Fluorescent Probes for Chemoselective Bioimaging. *Nat. Chem.* **4**, 973–984 (2012).
28. Wei, Y. *et al.* Pb(II) Metal-Organic Nanotubes Based On Cyclodextrins: Biphasic Synthesis, Structures and Properties. *Chem. Sci.* **3**, 2282–2287 (2012).
29. Mariappan, K. *et al.* Improved Selectivity for Pb(II) by Sulfur, Selenium and Tellurium Analogues of 1, 8-Anthraquinone-18-Crown-5: Synthesis, Spectroscopy, X-ray Crystallography and Computational Studies. *Dalton Trans.* **44**, 11774–11787 (2015).
30. Zhang, L. *et al.* A colorimetric and ratiometric fluorescent probe for the imaging of endogenous hydrogen sulphide in living cells and sulphide determination in mouse hippocampus. *Org. Biomol. Chem.* **12**, 5115–5125 (2014).
31. Wang, X. *et al.* A near-infrared ratiometric fluorescent probe for rapid and highly sensitive imaging of endogenous hydrogen sulfide in living cells. *Chem. Sci.* **4**, 2551–2556 (2013).
32. Miessler, G. L. *et al.* *Inorganic Chemistry* (5th Edition), Prentice Hall (2013).
33. Kellner, R. *Analytical Chemistry*, WILEY-VCH Verlag GmbH. (1988).
34. Nugent, J. W. *et al.* Spectroscopic, structural, and thermodynamic aspects of the stereochemically active lone pair on lead(II): Structure of the lead(II) dota complex. *Polyhedron.* **91**, 120–127 (2015).
35. Alcantara, D. *et al.* Fluorochrome-Functionalized Magnetic Nanoparticles for High-Sensitivity Monitoring of the Polymerase Chain Reaction by Magnetic Resonance. *Angew. Chem. Int. Ed.* **51**, 6904–6907 (2012).
36. Dean, J. A. *Lange's Handbook of Chemistry* 15th Ed. edition, McGraw-Hill, Inc. (1999).
37. Mustafina, A. N. *et al.* Hydrogen Sulfide Induces Hyperpolarization and Decreases the Exocytosis of Secretory Granules of Rat GH₃ Pituitary Tumor Cells. *Biochem. Biophys. Res. Commun.* **465**, 825–831 (2015).
38. Khader, H. *et al.* Overlap of Doxycycline Fluorescence with that of the Redox-Sensitive Intracellular Reporter roGFP. *J. Fluoresc.* **24**, 305–311 (2014).
39. Karton-Lifshin, N. *et al.* “Donor-Two-Acceptor” Dye Design: A Distinct Gateway to NIR Fluorescence. *J. Am. Chem. Soc.* **134**, 20412–20420 (2012).
40. Deniz, E., Sortino, S. & Raymo, F. M. Fluorescence Switching with a Photochromic Auxochrome. *J. Phys. Chem. Lett.* **1**, 3506–3509 (2010).
41. Hendrickx, J. *et al.* Location of the Hydroxyl Functions in Hydroxylated Metabolites of Nebivolol in Different Animal Species and Human Subjects as Determined by On-Line High-Performance Liquid Chromatography-Diode-Array Detection. *J. Chromatogr. A.* **729**, 341–354 (1996).
42. Karton-Lifshin, N. *et al.* A Unique Paradigm for a Turn-ON Near-Infrared Cyanine-Based Probe: Noninvasive Intravital Optical Imaging of Hydrogen Peroxide. *J. Am. Chem. Soc.* **133**, 10960–10965 (2011).
43. Yuan, C., Jin, Z. & Xu, X. Inclusion Complex of Astaxanthin with Hydroxypropyl- β -Cyclodextrin: UV, FTIR, ¹H NMR and Molecular Modeling Studies. *Carbohydr Polym.* **89**, 492–496 (2012).
44. Maheshwari, A., Sharma, M. & Sharma, D. Investigation of the Binding of Roxatidine Acetate Hydrochloride with Cyclomaltoheptaose (β -Cyclodextrin) Using IR and NMR Spectroscopy. *Carbohydr Res.* **346**, 1809–1813 (2011).
45. McNamara, M. *et al.* FT-IR and Raman Spectra of a Series of Metallo- β -Cyclodextrin Complexes. *J. Inclusion Phenomena and Molecular Recognition & Chemistry.* **10**, 485–495 (1991).
46. Skinner, W. M., Qian, G. & Buckley, A. N. Electronic Environments in Ni₃Pb₂S₂ (Shandite) and its Initial Oxidation in Air. *J. Solid State Chem.* **206**, 32–37 (2013).
47. Borrmann, H. *et al.* Trigonal Bipyramidal M₂Ch₃²⁻ (M = Sn, Pb; Ch = S, Se, Te) and TIMTe₃³⁻ Anions: Multinuclear Magnetic Resonance, Raman Spectroscopic, and Theoretical Studies, and the X-ray Crystal Structures of (2, 2, 2-crypt-K⁺)₃ TIPbTe₃³⁻-2en and (2,2,2-crypt-K⁺)₂Pb₂Ch₃²⁻-0.5en (Ch = S, Se). *Inorg. Chem.* **37**, 6656–6674 (1998).
48. Huang, M. *et al.* Synthesis of Semiconducting Polymer Microparticles as Solid Ionophore with Abundant Complexing Sites for Long-Life Pb(II) Sensors. *ACS Appl. Mater. Inter.* **6**, 22096–22107 (2014).

49. Samet, M. *et al.* Power of a Remote Hydrogen Bond Donor: Anion Recognition and Structural Consequences Revealed by IR Spectroscopy. *J. Org. Chem.* **80**, 1130–1135 (2015).
50. Zhang, C. H. *et al.* Au@Poly(N -Propargylamide) Nanoparticles: Preparation and Chiral Recognition. *Macromol. Rapid Comm.* **34**, 1319–1324 (2013).
51. Nagarkar, S. S. *et al.* Metal-Organic Framework Based Highly Selective Fluorescence *Turn-On* Probe for Hydrogen Sulphide. *Sci. Rep.* **4**, 7053–7058 (2014).
52. Choi, S. *et al.* Selective Detection of Acetone and Hydrogen Sulfide for the Diagnosis of Diabetes and Halitosis Using SnO₂ Nanofibers Functionalized with Reduced Graphene Oxide Nanosheets. *ACS Appl. Mater. Inter.* **6**, 2588–2597 (2014).
53. Qian, Y. *et al.* Selective Fluorescent Probes for Live-Cell Monitoring of Sulphide. *Nat. Commun.* **2**, 495–502 (2011).
54. Vivero-Escoto, J. L. *et al.* Mesoporous Silica Nanoparticles for Intracellular Controlled Drug Delivery. *Small*, **6**, 1952–1967 (2010).
55. Wang, X. *et al.* Lanthanide Metal-Organic Frameworks Containing a Novel Flexible Ligand for Luminescence Sensing of Small Organic Molecules and Selective Adsorption. *J. Mater. Chem. A*, **3**, 12777–12785 (2015).
56. Wu, Y. *et al.* Complexation of Polyoxometalates with Cyclodextrins. *J. Am. Chem. Soc.* **137**, 4111–4118 (2015).
57. Holcroft, J. M. *et al.* Carbohydrate-Mediated Purification of Petrochemicals. *J. Am. Chem. Soc.* **137**, 5706–5719 (2015).
58. Hou, X. *et al.* Tunable Solid-State Fluorescent Materials for Supramolecular Encryption. *Nat. Commun.* **6**, 6884–6892 (2015).
59. Wang, R. *et al.* A highly selective turn-on near-infrared fluorescent probe for hydrogen sulfide detection and imaging in living cells. *Chem. Commun.* **48**, 11757–11759 (2012).
60. Butler, A. R., Rutherford, T. J., Short, D. M. & Ridd, J. H. Tyrosine nitration and peroxynitrite (peroxynitrite) isomerisation: ¹⁵N CIDNP NMR studies. *Chem. Commun.* **7**, 669–670 (1997).

Acknowledgements

This work was supported by the NSFC (Grant Nos. 21371179, 21271117), NCET-11-0309, the Shandong Natural Science Fund for Distinguished Young Scholars (JQ201003), Shandong Provincial Natural Science Foundation (ZR2015BM005), the Fundamental Research Funds for the Central Universities (13CX05010A, 14CX02150A, 14CX06103A).

Author Contributions

X.L.X., D.F.S. and R.M.W. conceived and designed the experiments and co-wrote the paper. C.F.G., S.J.J. and H.X.D. synthesized the compound. X.L.X., J.X.W., Q.G.M. and L.L.Z. performed most of experiments and analyzed data. D.F.S., F.N.D. and H.X. analyzed the data and wrote the manuscript. All authors discussed the results and commented on the manuscript.

Additional Information

Supplementary information accompanies this paper at <http://www.nature.com/srep>

Competing financial interests: The authors declare no competing financial interests.

How to cite this article: Xin, X. *et al.* Cyclodextrin-Based Metal-Organic Nanotube as Fluorescent Probe for Selective *Turn-On* Detection of Hydrogen Sulfide in Living Cells Based on H₂S-Involved Coordination Mechanism. *Sci. Rep.* **6**, 21951; doi: 10.1038/srep21951 (2016).



This work is licensed under a Creative Commons Attribution 4.0 International License. The images or other third party material in this article are included in the article's Creative Commons license, unless indicated otherwise in the credit line; if the material is not included under the Creative Commons license, users will need to obtain permission from the license holder to reproduce the material. To view a copy of this license, visit <http://creativecommons.org/licenses/by/4.0/>